M. LOSERTOVÁ, M. ŠTAMBORSKÁ, J. LAPIN, V. MAREŠ

ISSN 0543-5846
METABK 55(4) 667-670 (2016)
UDC – UDK 669.15:669.295:620.17:539.382=111

COMPARISON OF DEFORMATION BEHAVIOR OF 316L STAINLESS STEEL AND Ti6Al4V ALLOY APPLIED IN TRAUMATOLOGY

Received – Prispjelo: 2015-11-23
Accepted – Prihvaćeno: 2016-03-25
Original Scientific Paper – Izvorni znanstveni rad

The comparative analysis of mechanical properties was performed for AISI 316L stainless steel and Ti6Al4V alloy using the digital image correlation (DIC) method. Both types of materials are commonly used for implants in traumatology. Tensile tests of the cylindrical tensile specimens were performed at room temperature and at an initial strain rate of 0,0025 s^{-1}. The strain analysis during tensile tests was carried out by means of Vic 2D image correlation software. Ti6Al4V alloy showed higher yield strength and tensile strength. The differences in the strain localization zones were observed.

Key words: stainless steel AISI 316L, titanium alloy Ti6Al4V, mechanical properties, digital image correlation (DIC), strain fields

INTRODUCTION

The austenitic stainless steel AISI 316L remains the most widely used metallic material for fracture fixation device in biomedicine due to its relatively low cost, ease of manufacturing, excellent formability, rupture and tensile strength at high temperatures, higher creep resistance and pitting and corrosion resistance to most chemicals [1, 2]. The differences between the Type 316L and the Type 316 consist in carbon content and in yield strength and tensile strength values. The lower carbon content in the 316L minimizes deleterious carbide precipitation as a result of the heat affecting process. Moreover, the 316L is non-hardenable by heat treatment; it shows typically slightly lower yield and tensile strengths and can be readily formed or drawn. Usual annealing treatment consists in heating to 1 038 - 1 149 °C followed by rapidly quenching.

The second most frequently used material in traumatology is Ti6Al4V alloy that is characterized by higher biocompatibility, lower Young‘s modulus and higher corrosion resistance in comparison to the 316L stainless steel. Mechanical properties and strain distribution in relation to microstructure resulting from mechanical and thermal treatment are important features influencing the reliability and safety of implants [3].

M. Losertová, M. Štamborská, VŠB-Technical University Ostrava, Faculty of Metallurgy and Materials Engineering, Czech Republic
J. Lapin, Institute of Materials & Machine Mechanics Slovak Academy of Sciences, Bratislava, Slovakia
V. Mareš, VŠB-Technical University Ostrava, Center of Advanced Innovation Technologies, Czech Republic

In this work, the tensile tests of AISI 316L stainless steel and Ti6Al4V were realized at room temperature in order to compare the deformation behavior using strain analysis. In the experimental analysis of plastic deformation on the surface of specimens, it is advantageous to use contactless displacement sensing methods, allowing obtaining of deformation fields in pre-selected areas. The digital image correlation (DIC) is one of the most advanced optical methods of displacement sensing and subsequent determination of strains on the surface of examined objects. The strain fields are calculated from the displacement fields by the Vic 2D program [4].

EXPERIMENTAL PROCEDURES

The study of deformation behavior was performed on AISI 316L stainless steel and Ti6Al4V alloy. Six cylindrical tensile test specimens with a gauge length of 28 mm and gauge diameter of 5 mm were prepared from swaged bars of both materials supplied by the company MEDIN, a.s. (Czech Republic).

The initial microstructure of both alloys was observed using optical microscopy (OM). After grinding and polishing the transversal and longitudinal sections were etched in solutions composed of 1 HNO_3 : 10 HCl : 10 H_2O and 2 HF : 4 HNO_3 : 80 H_2O, for the 316L stainless steel and Ti6Al4V alloy, respectively.

The tensile tests were carried out at an initial strain rate of 0,0025 s^{-1} on the experimental setup consisting of Zwick / Roel Z150 tensile machine with hydraulic grips and with the Canon 5D Mark II camera.

The strains fields distribution was evaluated using image correlation software Vic 2D. The principle of the

method is based on scanning of stochastic black and white spotted pattern created on the surface of the examined object, for example by spraying black paint on white background. The observed area is divided by virtual grid into smaller sub-areas called facets, so that each of them contains a characteristic part, with sufficient contrast of the pattern. Based on the correlation of corresponding facets before and after deformation, the displacements of the individual points and strain fields are determined.

In the case of plane image correlations, the object deformations are determined by an observation through one camera directed perpendicularly to the surface of the object. This procedure allows determination of the deformation of the object in a level parallel to the image level of the camera [5, 6].

RESULTS AND DISCUSSION

The austenitic microstructure of AISI 316L steel in the as-received state was formed of fine grains with twins that corresponded to the pre-deformation of the material during its processing by cold forming. Twinning is generally observed as a deformation mechanism that is activated at high strain rates [7]. Figure 1 shows the transversal section with fine grains of 19 μm in the mean size (Figure 1 a) and a longitudinal section with elongated grains in the direction of swaging (Figure 1 b).

Figure 2 represents the fine-grained microstructure of Ti6Al4V alloy in the as-received state. The transversal and longitudinal sections in Figures 2 a and 2 b, respectively, show very fine equiaxed grains of alpha phase with size under 5 μm (white) and alpha and beta lamellar grains (dark grey) that are elongated in longitudinal direction resulting from hot swaging followed by annealing.

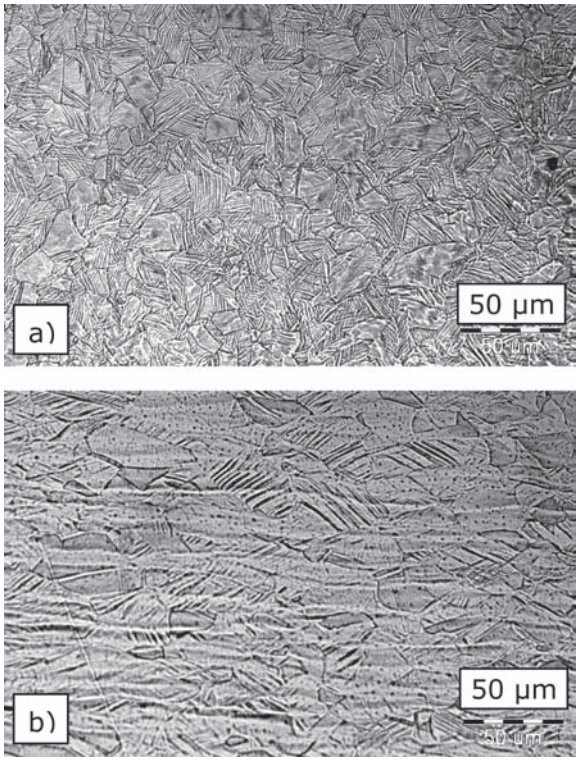

Figure 1 Fine-grained microstructure of austenitic 316L in as-received state: a) transversal and b) longitudinal sections.

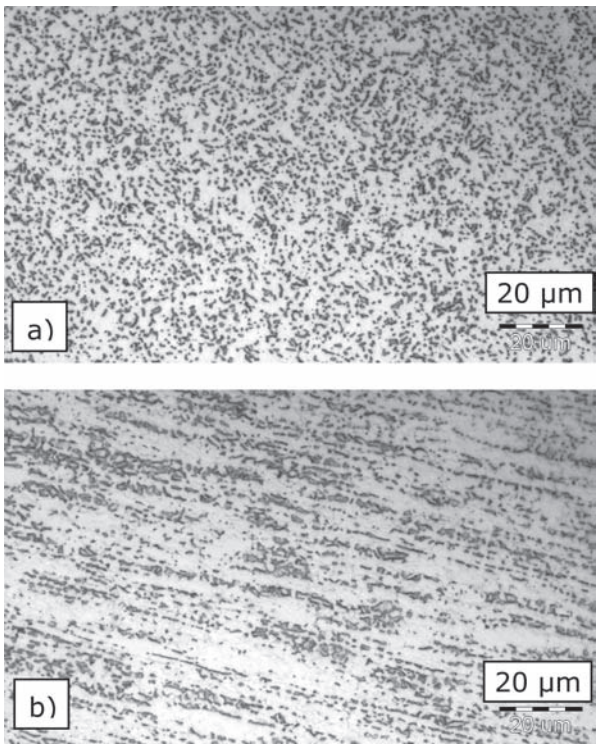

Figure 2 Fine-grained microstructure of Ti6Al4V in asreceived state: a) transversal and b) longitudinal sections.

Table 1 summarizes values of Young's modulus (E / GPa), 0,2 % offset yield strength (R_e / MPa), tensile strength (R_m / MPa) and elongation (A_5 / %) for AISI 316L steel and Ti6Al4V measured by the standard uniaxial tensile test. Comparison of the mechanical properties and Young's modulus confirms that Ti6Al4V alloy is more suitable for traumatology implants in view of biomechanical compatibility [8].

Figure 3 shows the typical tensile engineering stress - strain curves of the AISI 316L steel and Ti6Al4V alloy specimens, respectively, tested to the fracture. As it can be seen in figure, the deformation behavior of both materials with similar high strength characteristics significantly differs under loading. The feature of tensile curves points at a different work hardening.

Table 1 **Mechanical properties of AISI 316L and Ti6Al4V.**

		E / GPa	R_e / MPa	R_m / MPa	A_5 / %
AISI 316 L	1	212	904	979	15
	2	209	887	972	19
	3	208	885	980	16
Average value		210	892	977	17
Ti6Al4V	4	106	921	1 031	17
	5	106	920	1 037	17
	6	105	915	1 034	13
Average value		106	919	1 034	16

Indeed, for AISI 316L steel a work hardening rate, Q / MPa, that was derived for uniform deformation from true stresses σ_t vs. true strains ε_t as a function [9, 10]:

$$\Theta = \frac{d\sigma_t}{d\varepsilon_t} \quad (1)$$

drops rapidly with a strain in the true strain range from 0 to 0,01 as the deformation approaches the plastic instability point and then decreases slowly with great perturbations toward necking. Unlike AISI 316L steel the samples of Ti6Al4V alloy exhibit almost linear decrease of the work hardening rate with a strain in the uniform deformation region. Evolution of the work hardening rate with the strain is shown in Figure 4.

Despite the diverse microstructures, both materials are hardened with similar hardening capacity, H_c / -, that is defined as a ratio of the R_m to the R_e [11]. The values of 1,095 and 1,125 correspond to fine twinned grains for AISI 316L steel and fine-grained Ti6Al4V alloy, respectively.

As it was mentioned above, the Vic 2D software enables the calculation of strain fields from the experimentally measured displacement fields during the entire tensile tests. The distribution of strains shown in Figures 5 and 6 corresponds to the last stage of the tensile test when necking initiates. Figure 5 displays the strain fields ε_x, ε_y and γ_{xy} measured by the 2D DIC method on the surface of the AISI 316L. Figures 5 a and 5 b illustrate that high local values of ε_x strain up to 80 % and ε_y strain up - 50 % are achieved in the central region of displaced 2D visualization, respectively. The values of γ_{xy} shear strain range from more than - 10 % to 10 %, as seen in Figure 5 c.

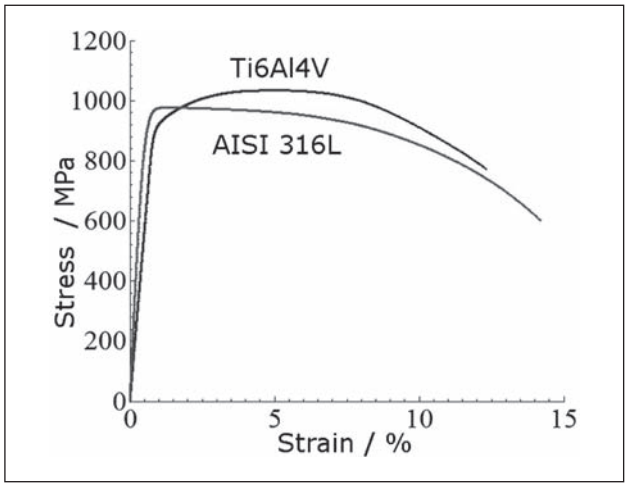

Figure 3 Engineering stress-strain curves for AISI 316L stainless steel and Ti6Al4V alloy.

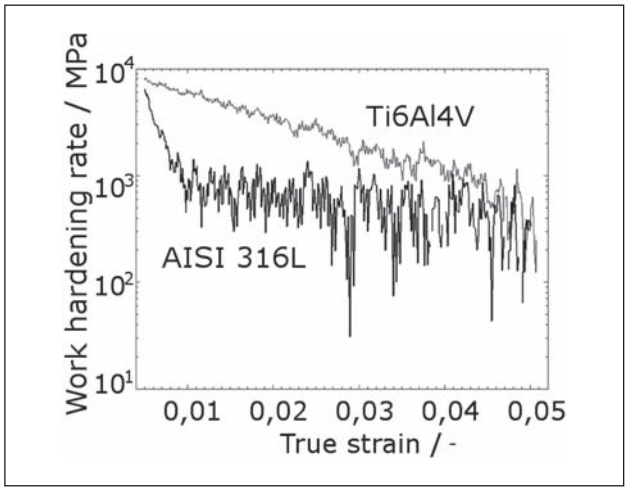

Figure 4 Dependence of work hardening rate on true strain calculated on the assumption of uniform deformation of the tensile specimen.

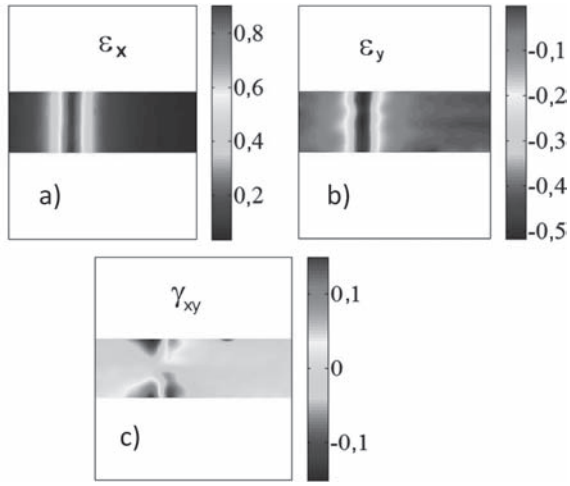

Figure 5 Strain fields a) ε_x / -, b) ε_y / - and c) γ_{xy} / - obtained by DIC for AISI 316L.

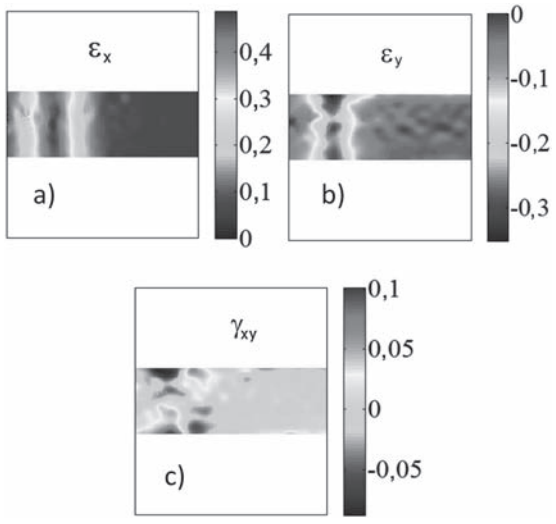

Figure 6 Strain fields a) ε_x / -, b) ε_y / - and c) γ_{xy} / - obtained by DIC for Ti6Al4V.

The strain fields ε_x, ε_y and γ_{xy} measured by the 2D DIC method on the surface of the Ti6Al4V alloy are shown in Figure 6. Unlike the strains fields of the stainless steel, the ε_x and ε_y strains for Ti6Al4V alloy reach lower values, as seen in Figures 6 a and 6 b. In the central region of the displaced 2D visualization, the ε_x and ε_y strains achieved the highest local values up to 40 % and - 30 %, respectively. The values of γ_{xy} shear strain range from - 10 % to 10 %, as seen in Figure 6 c.

CONCLUSIONS

Based on the results of comparative tensile behavior and microstructure analysis of the AISI 316L stainless steel and Ti6Al4V alloy it is possible to draw the following conclusions:

The initial state of both alloys was characterized by very fine microstructure due to previous swaging. Owing to this the mechanical properties reached high values in the asreceived state.

Additional data measured using DIC method during tensile testing were used for calculation of the work hardening rates during uniform deformation from true stresses and true strains.

The work hardening behavior of the 316L steel differs from that of Ti6Al4V. While the hardening capacity seems to be similar for both materials, the work hardening rate decreases rapidly with strain for the 316L steel.

The DIC method allowed observation of the differences in the strain values in the middle of the strain localization zone.

The method allowed us to determine the distribution and amount of deformation, at which the samples were fractured, but also to detect locations of defects or microstructure heterogeneities formed during production of materials.

Acknowledgements

This article has been elaborated within the framework of the Project No. LO1203 «Regional Materials Science and Technology Centre - Feasibility Program» funded by the Ministry of Education, Youth and Sports of the Czech Republic, the Project No. TA03010804 financed by Technology Agency of the Czech Republic and the Project RRC/07/2014 „Support research and development in the Moravian - Silesian Region 2014 DT1 -Research teams“, financed from the budget of the Moravian - Silesian Region.

REFERENCES

[1] J. D. Enderle, J. D. Bronzino, S. M. Blanchard, Introduction to Biomedical Engineering. (Second ed.), Elsevier Academic Press, Amsterdam, 2005, 1253 p.

[2] J. V. Sloten, L. Labey, R. Van Audekercke, G. Van der Perre, Materials selection and design for orthopedic implants with improved long-term performance, Biomaterials 19 (1998) 16, 1455–1459.

[3] R. K. Nalla, B. L. Boyce, J. P. Campbell, J. O. Peters, R. O. Ritchie, Influence of microstructure on high cycle fatigue of Ti – 6Al – 4V: bimodal vs. lamellar structure, Metall. Mater. Trans. 33A (2002), 899–918.

[4] M. Hagara, F. Šimčák, M. Kalina, The knowledge acquired by using of optical methods by strain fields investigation, Applied Mechanics and Materials 486 (2014), 141-146.

[5] F. Šimčák, M. Štamborská, R. Huňady, Deformation of materials by using digital image correlation Chemické Listy 105 (2011) 4, 564-567.

[6] M. Rossi, F. Pierron, M. Štamborská, F. Šimčák, Identification of the Anisotropic Plastic Behaviour of Sheet Metals at Large Strains, Experimental and Applied Mechanics (2013), 229-235. DOI: 10.1007/978-1-4614-4226-4_27.

[7] J.W. Christian, S. Mahajan, Deformation twinning, Progres in Material Science 39 (1995), 1-157.

[8] M. Geetha, A.K. Singh, R. Asokamani, Ti based biomaterials, the ultimate choice for orthopaedic implants – A review. Progress in Materials Science 54 (2009), 397-425

[9] X. Cao, M. Jahazi, H. Al-Kazzaz, M. Medraj, Modelling of work-hardening behaviour for laser welded magnesium alloy, Int. J. Mat. Res. 99 (2008) 2, 216-221

[10] S.M. Chowdhury, D.L. Chen, S.D. Bhole, X. Cao, E. Powidajko, D.C. Weckman, Y. Zhou, Tensile properties and strain-hardening behavior of double-sided arc welded and friction stir welded AZ31B magnesium alloy, Materials Science and Engineering A 527 (2010), 2951-2961.

[11] N. Afrin, D.L. Chen, X. Cao, M. Jahazi, Strain hardening behavior of a friction stir welded magnesium alloy, Scripta Mater. 57 (2007), 1004-1007.

Note: Responsible translator for the English language is Boris Škandera, Czech Republic